In silico screening of naturally occurring coumarin derivatives for the inhibition of the main protease of SARS-CoV-2

Sona Lyndem[$], Sharat Sarmah[$], Sourav Das and Atanu Singha Roy*

Department of Chemistry, National Institute of Technology Meghalaya, Shillong 793003, India

[$] Equal contribution

Running head title: Coumarins as potential inhibitors of SARS-CoV-2

***Corresponding Author:** Atanu Singha Roy

Tel.: +91 364−2501294

Fax: +91 364−2501113

Email: singharoyatanu@gmail.com; asroy86@nitm.ac.in

Abstract

The dissemination of a novel corona virus, SARS-CoV-2, through rapid human to human transmission has led to a global health emergency. The lack of a vaccine or medication for effective treatment of this disease has made it imperative for developing novel drug discovery approaches. Repurposing of drugs is one such method currently being used to tackle the viral infection. The genome of SARS-CoV-2 replicates due to the functioning of a main protease called M^{pro}. By targeting the active site of M^{pro} with potential inhibitors, this could prevent viral replication from taking place. Blind docking technique was used to investigate the interactions between 29 naturally occurring coumarin compounds and SARS-CoV-2 main protease, M^{pro}, out of which 17 coumarin compounds were seen to bind to the active site through the interaction with the catalytic dyad, His41 and Cys145, along with other neighbouring residues. On comparing the ΔG values of the coumarins bound to the active site of M^{pro}, corymbocoumarin belonging to the class pyranocoumarins, methylgalbanate belonging to the class simple coumarins and heraclenol belonging to the class furanocoumarins, displayed best binding efficiency and could be considered as potential M^{pro} protease inhibitors. Preliminary screening of these naturally occurring coumarin compounds as potential SARS-CoV-2 replication inhibitors acts as a stepping stone for further *in vitro* and *in vivo* experimental investigation and analytical validation.

Keywords: Coumarins; SARS-CoV-2 M^{pro}; molecular docking, active site; anti-viral.

1. Introduction

The year 2020 is continuing to be a year where extreme pressure is being put on the health care system of nations all over with world with the outbreak of a novel corona virus, SARS-CoV-2. This novel corona virus causing SARS-like acute respiratory syndrome was first reported in late December 2019 in the Chinese city of Wuhan, Hubei Province (Wang et al., 2020). Because this disease caused by SARS-CoV-2 was discovered in the end of 2019, the World Health Organisation (WHO) on 12th February 2020 named this disease as COVID-19 which stands for coronavirus disease 2019 (https://www.who.int/emergencies/diseases/novel-coronavirus-2019/situation-reports). With the rapid spread of the COVID-19 disease beyond the borders of China, leading to a sustained risk of further global spread, on 11th March 2020 the WHO declared COVID-19 as a global pandemic (Cucinotta & Vanelli, 2020). Despite various actions being taken by global governments to contain this virus, the total number of global COVID-19 positive cases stands at 31,75,207 including 2,24,172 deaths as of 1st May 2020, reported by WHO (https://www.who.int/emergencies/diseases/novel-coronavirus-2019/situation-reports).

The SARS-CoV-2 still remains a mystery in terms of its origin, its transmission to human beings and most importantly, its treatment. The ease at which human to human transmission of this virus takes place has put global nations to an economic and social halt. Despite the collaborative efforts of researchers all over the world, a suitable and effective drug candidate or vaccine to treat patients or to mitigate virus transmission is still unavailable. With a time constraint to combat the SARS-CoV-2 virus, efforts are now being put into repurposing of existing drugs (Muralidharan et al., 2020). Anti-malarial drugs such as hydroxychloroquine and chloroquine have been approved by the FDA to be tested against COVID-19 (Dong et al., 2020). To name a few, anti-viral drug such as flavilavir is being used in China to treat patients with COVID-19 symptoms (Li et al., 2020). Darunavir an anti-retroviral protease inhibitor is reported to inhibit SARS-CoV-2 replication (Dong et al., 2020). Infected patients

treated with anti-retroviral protease inhibitors lopinavir/ritonavir have been associated with improvements (Chan et al., 2003; Chu et al., 2004). Now many drugs are being repurposed, through preliminary screening, in order to study their anti-SARS-CoV-2 replication efficiency.

Replication in SARS-CoV-2 is aided by a chymotrypsin-fold proteinase called main protease (M^{pro} or $3CL^{pro}$) (Anand et al., 2003; Boopathi et al., 2020). M^{pro} plays an indispensible role in processing polyproteins at 11 cleavage sites in order to generate critical non-structural proteins such as helicase, methyl transferase and RNA dependent RNA polymerase, all important for viral replication (Cui et al., 2019). Thus M^{pro} is considered an attractive drug target to block its proteolytic action which will ultimately lead to an inhibition of viral replication (Khan et al., 2020; Morse et al., 2020; Wu Y-S, 2006). The crystal structure of M^{pro} has been published and made available since February 2020. His41 and Cys145, the catalytic dyad, is found at the junction of domain I and Domain II of M^{pro} and is responsible for its catalytic activity (Zhang et al., 2020). The crystal structure of M^{pro} used in this study (PDB ID. 6Y84) is depicted in Figure 1 in which active site residues have been highlighted.

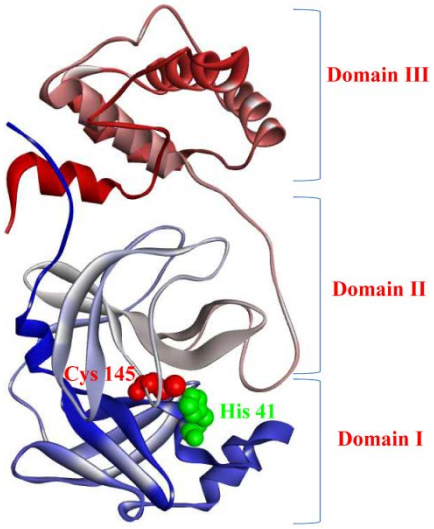

Figure 1. The crystal structure of the main protease M^{pro} of SARS-CoV-2. (PDB ID. 6Y84)

Preliminary screening of drugs using *in silico* methods have proved to be useful in meeting challenges of discovering potential candidates. Along with synthetic and semi synthetic drugs

being used to target many viral proteins to inhibit viral spread, natural compounds are also being screened in a similar manner. Natural compounds are structurally and chemically diverse, with least side effects and toxicity, making them valuable contenders in the fight against COVID-19. Reports suggest that 45% of the best selling drugs have been derived from natural products or their derivatives (Lahlou, 2013). With this knowledge, naturally occurring coumarin compounds were selected and screened out as potential M^{pro} inhibitors using molecular docking studies. Various substituents and conjugates present on the central bicyclic structure of coumarins bestow on it many biological effects and potential therapeutic and pharmacological properties. In addition, their stability, low side effects and toxicity, oral bioavailability and broad spectrum have made coumarins find a place in the medicinal field (Wang H, 2009). Numerous studies have reported anti-viral activity of naturally occurring coumarins inhibiting the functioning of viral proteins such as proteases, integrase, reverse transcriptase, DNA polymerase and also in preventing viral entry(Hassan et al., 2016; Mishra et al., 2020). For example, coumarins such as oxypeucedanin, heraclenol, pranferol, and xanthotoxin has been known to exhibit anti-HIV activity (Zhou et al., 2000). Structurally similar coumarin compounds, psoralen, saxalin and bergapten have been reported to prevent HIV replication (Shikishima et al., 2001). Also, mesuol and isomesuol have been found to suppress HIV replication in Jurkat T cells (Márquez et al., 2005). Rutamarin, a naturally occurring furanocoumarin, and kellerin, a sesquiterpene coumarin, were reported to be anti-HSV agents (Ghannadi et al., 2014; Xu et al., 2014)

In this study, molecular docking method was used to study the interactions between naturally occurring coumarin compounds and the SARS-CoV-2 main protease, M^{pro}. We reported that a total of 17 coumarin compounds could interact with the catalaytic dyad in the active site of M^{pro}, namely, mesuol (4441487), pabulenol (446229), pranferol (140461), saxalin (158533), seselin (61531) xanthotoxin (3971), heraclenol (66005), kellerin (40580807), oxypeucedanin (141075), rutamarin (25094), anomalin (4477595), esculin (4444765), methylgalbanate

(5428912), isofraxidin (4477107), osthole (9811) sphondin (97199) and corymbocoumarin (969471). The numbers indicated in bracket for the first sixteen coumarin compounds depicts their ChemSpider ID and the number for the last coumarin, corymbocoumarin, signifies its PubChem ID.

2. Materials and Methods

Finding potential lead compounds using *in silico* methods can help to reduce the time and resources involved in the drug development process. By conducting molecular docking studies, potential drug candidates can be screen out from a large number of compounds by studying their interactions with biological molecules.

In this study, blind docking analysis was carried out between some naturally occurring coumarins and the main protease, M^{pro}, of SARS-CoV-2.

2.1 Preparation of M^{pro} for docking studies

The crystal structure of the main protease M^{pro} (PDB ID. 6Y84) of SARS-CoV-2 was retrieved from RCSB Protein Data Bank (PDB) (Owen, 2020). The main protease obtained consisted of a dimer of two homologous amino acid chain, chain A and chain B, in which chain A was used as a target for molecular docking. Before docking studies was carried out the target molecule was prepared which involved the removal of water molecules using PyMOL(Schrodinger, 2017).

2.2 Preparation of ligands

Sixteen of the coumarin ligands were downloaded in the form of 3D coordinates from Chemspider (www.chemspider.com) and one coumarin ligand from PubChem (www.pubchem.ncbi.nlm.nih.gov) in .mol format. ArgusLab using PM3 methods was then used to conduct energy optimization of the ligands.

2.3 Molecular docking and visualization

The final M^{pro} PBD file and the geometry optimised ligands structures were uploaded onto the SWISSDOCK server (http://www.swissdock.ch/docking) for molecular docking analysis. SwissDock is based on the docking software EADock DSS, whose algorithm consists of generating a number of binding modes either through local docking or blind docking, estimates CHARM (Chemistry at HARvard Macromolecular Mechanics)energy on a grid and producing clustered binding modes with most favourable binding energies (Grosdidier et al., 2011). Analysis is carried out on the docked pose which has the minimum fullfitness score. Visualization of the results obtained from SWISSDOCK was done in a molecular visualization tool, UCFS Chimera (Pettersen et al., 2004). The dock poses and 2D interaction plots were then prepared using Discovery Studio Visualizer (BIOVIA., 2019). An online server (http://cib.cf.ocha.ac.jp/bitool/ASA/) was used to determine the changes in the accessible surface area of the main protease when bound to the ligand. Finally, APBS plugin of PyMOL was used to determine the electrostatic surface potential(Schrodinger, 2017).

2.4 Drug-likeliness studies

Lipinski's rule of five dictates four parameters (molecular weight <500 Da, no of hydrogen bond donors should be less than 5, no. of hydrogen bond acceptors should be less than 10 and log *P* should not be greater than 5) in order for a compound to be considered a potential drug. The coumarin ligands were uploaded on to SWISSADME (www.swissadme.ch/index.php) server to obtain the above mentioned five parameters of Lipinski's rule. The chemical structures, chemical formula and the Lipinski's rule of five parameters of the ligands have been provided in Table S1 (Supplementary Information).

3. Results and Discussion

In order to tackle the spread of COVID-19 infection, a promising mechanism would be to inhibit SARS-CoV-2 main protease, M^{pro}, which is critical for viral replication. Keeping this in mind, SWISSDOCK, an online molecular docking tool, was used to study the molecular interactions between naturally occurring coumarin compounds and the catalytic residues of

the active site of SARS-CoV-2's main protease, M^{pro}. The SWISSDOCK server also provided the binding modes of these ligands (coumarin compounds) which were listed according to their best fullfitness score. The minimum fullfitness score, for each ligand, with its corresponding minimum fullfitness score has been tabulated in Table 1.

Table 1. The minimum fullfitness score and the estimated Δ*G* for the interaction of coumarin derivatives with M^{pro}.

Sl No.	Structural Class	Compounds	Fullfitness score (kcal/mol)	Estimated Δ*G* (kcal/mol)
1	Simple Coumarins	Mesuol	-1202.47	-7.38
		Isofraxidin	-1195.52	-7.00
		Osthole	-1222.57	-7.24
		Methylgalbanate	-1223.49	-8.30
		Esculin	-1153.26	-7.74
		Kellerin	-1194.95	-8.18
2	Furanocoumarins	Rutamarin	-1204.09	-7.63
		Heraclenol	-1183.78	-8.20
		Oxypeucedanin	-988.57	-7.26
		Saxalin	-1194.32	-7.14
		Pabulenol	-1203.79	-7.42
		Pranferol	-1203.78	-7.16
		Xanthotoxin	-1204.35	-6.80
		Sphondin	-1210.09	-6.94
3	Pyranocoumarins	Seselin	-1201.05	-7.00
		Anomalin	-1206.64	-8.18
		Corymbocoumarin	-1207.28	-8.57

3.1 Docking studies for Simple Coumarins with SARS-CoV-2 M^{pro}

Mesuol, isofraxidin, methylgalbanate, esculin, osthole and kellerin, falling under the class of simple coumarins, were seen to bind to the active site of M^{pro} as illustrated by their respective docked poses along with their corresponding 2D interaction plots (Figure 2). Mesuol, a reported anti-viral agent known to inhibit HIV replication(Marquez et al., 2005), interacted with one of the catalytic dyad residue, His41, in the active site of M^{pro}, through π-alkyl interaction. Similar type of interaction was also seen between Cys44, Met49 of M^{pro} and mesuol. Formation of a hydrogen bond between Glu166 and mesuol along with van der Waals interactions with other residues, including Cys145, was also depicted in the 2D

interaction plot (Figure 2a). Isofraxidin was seen to interact with the active site of M^{pro} through hydrogen bonding with His164, π-alkyl interaction with Met165, carbon hydrogen bond with Gln189, π-donor hydrogen bond with Glu166 and non-covalent van der Waals interaction with other surrounding residues (Figure 2b). A stable interaction was also noted through the formation of a hydrogen bond between the naturally occurring coumarin, osthole, and Gly143 of M^{pro}. The 2D interaction plot also displayed other interactions such as alkyl hydrophobic interactions with Cys145 and His163 and π-alkyl interactions with Cys145 and Met49 (Figure 2c). Methylgalbanate formed numerous non covalent interactions with residues present in the active site of M^{pro} such as alkyl hydrophobic interaction with Cys145, His41, His163, Met165 and Leu167, π-alkyl interaction with Cys145, carbon hydrogen bond with Asn142 and Glu166 and finally few van der Waal interactions with surrounding residues (Figure 2d). The catalytic dyad, His 41 and Cys145, of M^{pro} interacts with esculin through carbon hydrogen bonding and π-sulphur interaction respectively. Esculin also formed hydrogen bonds with Glu166 and Gly143, carbon hydrogen bonds with Met165 and Asn142 and non-covalent van der Waals interaction with nearby residues of M^{pro} (Figure 2e). Kellerin, a coumarin with reported anti-viral activity, stabilised the active site of M^{pro} through non covalent interactions such as carbon hydrogen bond with Asn142 and Met165, alkyl hydrophobic interactions with His41 and Cys145, π-alkyl interaction with Cys145 and van der Waals interaction with corresponding amino acids (Figure 2f). The estimated free energy of binding, represented by ΔG, which signifies the binding affinity of the above mentioned naturally occurring coumarin compounds towards M^{pro}, was arranged in ascending order starting with methylgalbanate (-8.30 kcal/mol), kellerin (-8.18kcal/mol), esculin (-7.74 kcal/mol), mesuol (-7.38 kcal/mol), osthole (-7.24 kcal/mol) and finally isofraxidin (-7.00 kcal/mol). Figure 5a represents the electrostatic surface potential of the binding site of M^{pro} along with all the six simple coumarin compounds.

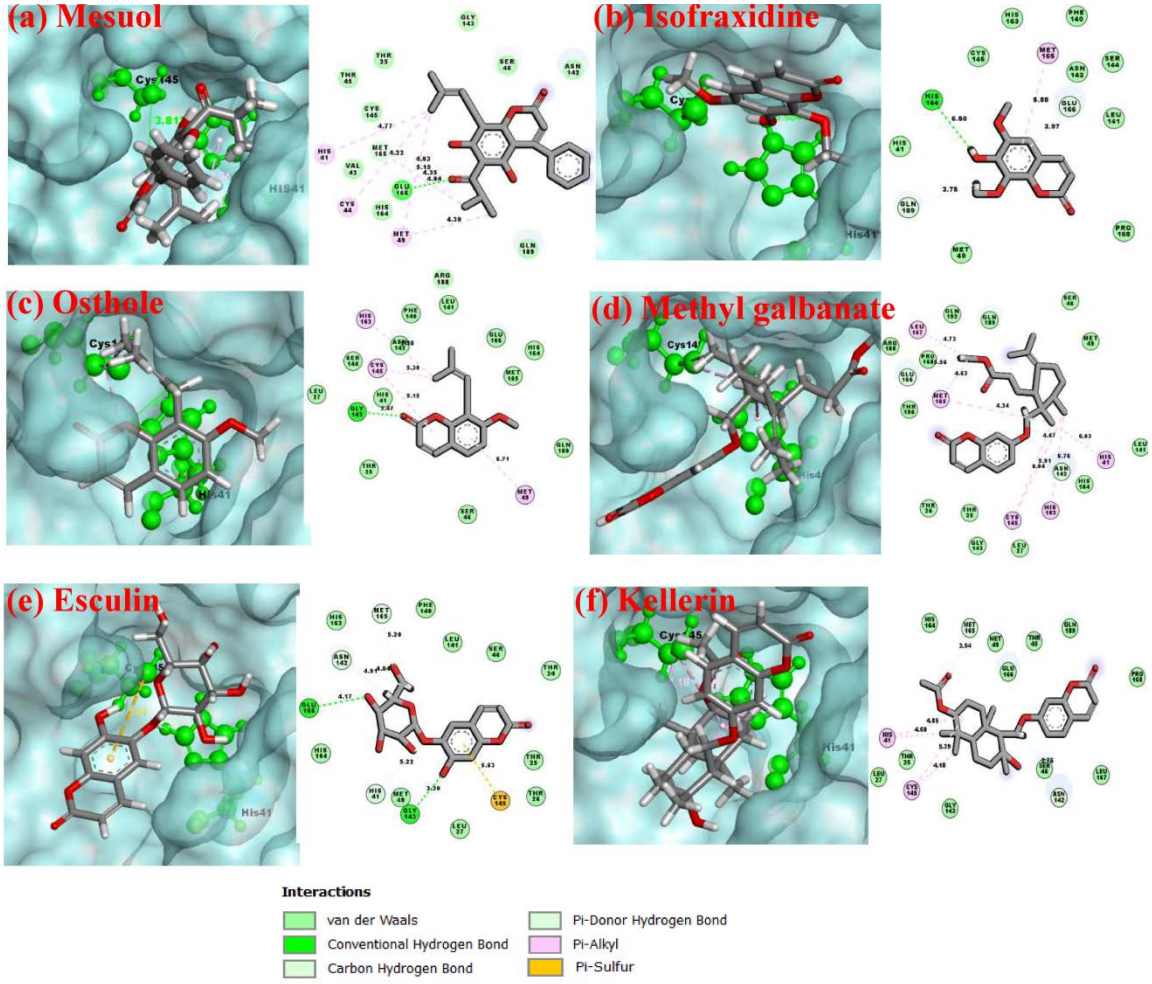

Figure 2. The minimum energy docked poses of the simple coumarin derivatives (a) mesuol, (b) isofraxidin, (c) osthole, (d) methylgalbanate, (e) esculin and (f) kellerin with 6Y84 with their corresponding 2-D interaction diagrams.

3.2 Docking studies for Furanocoumarins with SARS-CoV-2 M^{pro}

The docked poses of minimum energy of eight furanocoumarin compounds used in this study along with their 2D interaction plots are represented in Figure 3. Rutamarin, with reported anti-Herpes Simplex Virus (HSV) properties (Xu et al., 2014), interacted with the a number of residues present in the active site of M^{pro} through hydrogen bond formation with Ser46 and Glu166, alkyl hydrophobic interactions with His41, Met165 and Met49, π-alkyl interactions with Cys145 and His41, carbon hydrogen bond formation with Thr45 and van der Waals interaction with neighbouring residues (Figure 3a). Heraclenol formed hydrogen bonds with His41 and Ser144, carbon hydrogen bonds with Asn142, π-alkyl interactions with Cys145,

Met145 and Met49, π-donor hydrogen bond with Glu166 and van der Waals interaction with corresponding residues in order to stabilise the active site of M^{pro} (Figure 3b). Non covalent interactions was also seen between oxypeucedanin and M^{pro} active site residues through the formation of hydrogen bond with Gly143, carbon hydrogen bonds with His41, Cys44 and Asn142, alkyl hydrophobic interactions with Cys145, His41and Leu27, π-alkyl interaction with Met49 and van der Waals interaction with other residues as depicted in Figure 3c. Saxalin stabilized the active site of M^{pro} through carbon hydrogen bond formation with Leu141 and His41, π-donor hydrogen bond formation with Glu166, π-sigma interaction with His41, alkyl hydrophobic interaction with His41 and Met49, π-alkyl interaction with Met165, π-sulphur interaction with Cys145 and van der Waals interaction with nearby residues (Figure 3d). A number of interactions were witnessed between pabulenol and the residues of the active site of M^{pro} (Figure 3e). Hydrogen bonding of pabulenol with Leu141, π-sulphur interaction with Cys145, π-alkyl interaction with His163 and Met49 and carbon hydrogen bonding with Asn142. Van der Waals interactions with adjoining residues also helped to stabilise the interaction between pabulenol and M^{pro}. Another furanocoumarin, pranferol interacted with active site M^{pro} through the formation of a hydrogen bond with Glu166, π-alkyl interactions with Pro168 and Met165, alkyl hydrophobic interaction with Pro168, carbon hydrogen bonding with Thr190 and Gln189 and van der Waals forces was also a very dominant interaction present (Figure 3f). Xanthotoxin underwent a number of non-covalent interactions to stabilize the active site of M^{pro}. Residues located in the active site such as Gly143 and Glu166 formed hydrogen bonds with xanthotoxin, Cys145 formed π-sulphur type of interaction, Met165 formed π-alkyl interaction, Glu166 formed a carbon hydrogen bond with xanthotoxin and van der Waals interactions among corresponding residues was also present (Figure 3g). On the other hand, sphondin stabilised the active site of M^{pro} through the formation of carbon hydrogen bonds with His163, Leu141 and Asn142, π-alkyl interactions with Cys145, Met165 and Met49 and also through van der Waals interactions with adjoining

amino acid residues located in the active site (Figure 3h). The Δ*G* values, from Table 1, of the above mentioned furanocoumarins were compared and it was seen that heraclenol (-8.20 kcal/mol) had the most negative Δ*G* value followed by rutamarin (-7.63 kcal/mol), pabulenol (-7.42 kcal/mol), peucedanin (-7.26 kcal/mol), pranferol (-7.16 kcal/mol), saxalin (-7.14 kcal/mol), sphondin (-6.94 kcal/mol) and lastly followed by xanthotoxin (-6.80 kcal/mol). Finally, Figure 5b depicts the electrostatic surface potential of the binding site of M^{pro} with the synchronous presence of the eight furanocoumarin compounds.

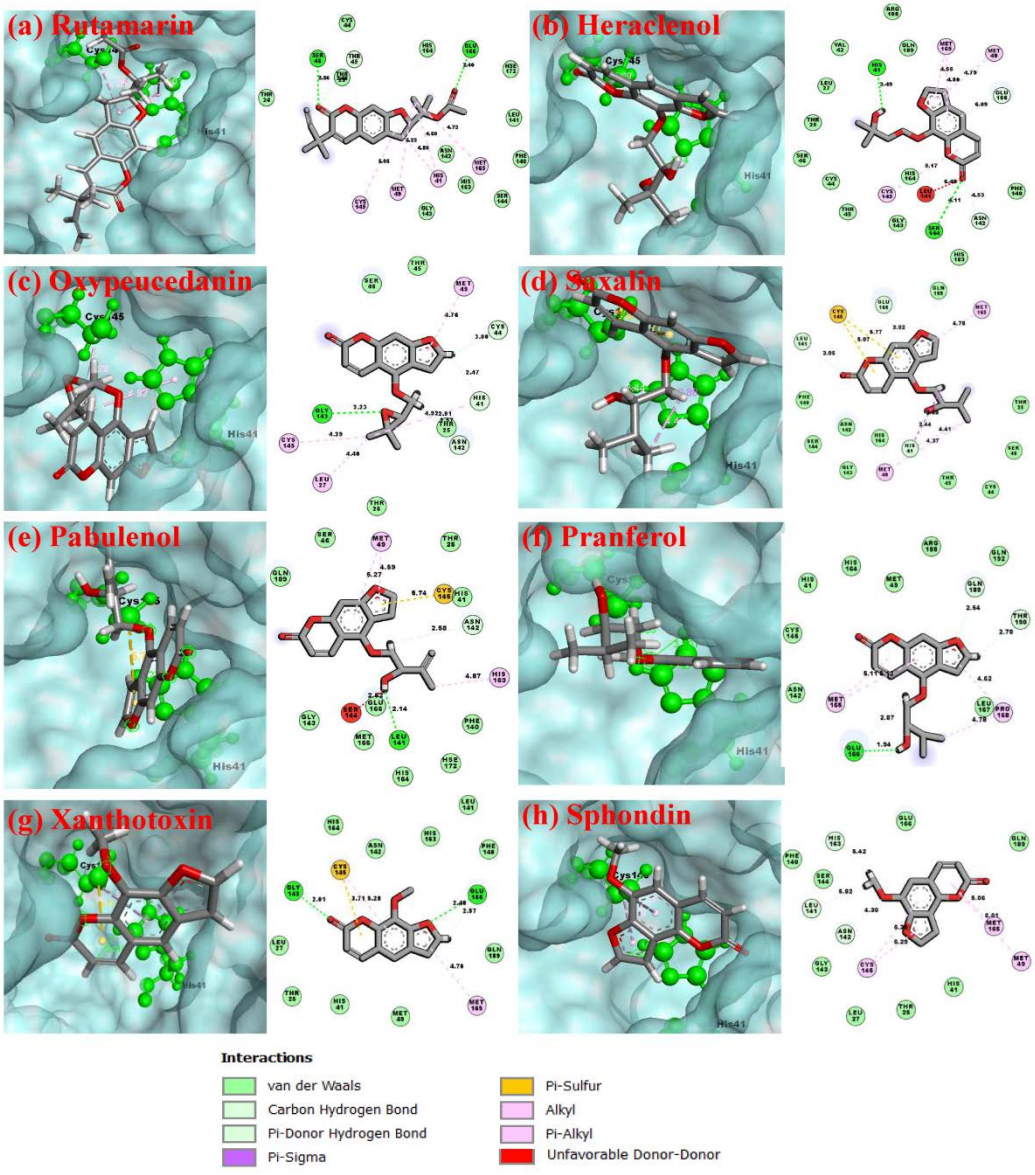

Figure 3. The minimum energy docked poses of the furanocoumarin derivatives (a) rutamarin, (b) heraclenol, (c) oxypeucedanin, (d) saxalin, (e) pabulenol, (f) pranferol, (g) xanthotoxin and (h) sphondin with 6Y84 with their corresponding 2-D interaction diagrams.

3.3 Docking studies for Pyranocoumarins with SARS-CoV-2 M^{pro}

Three pyranocoumarins, seselin, anomalin and corymbocoumarin, were docked on the active site of SARS-CoV-2 M^{pro} protease as illustrated in Figure 4 along with their 2-D interaction plot. Seselin interacted with the amino acid residues found in the active site of M^{pro} through the formation of a hydrogen bond with Gly143, π-alkyl interaction with Cys145, His41 and Met165, alkyl hydrophobic interactions with His41, Cys145and Leu27 and finally van der Waals interactions were also seen to interact with corresponding residues (Figure 4a). Many con-covalent interactions between anomalin and M^{pro} helped to stabilise this interaction. Alkyl hydrophobic interactions with His41, Met49, Cys145, Met165 and Pro168, π-alkyl interaction with His41, π-anion interaction with Glu166 and van der Waals interaction with many surrounding residues were among such stabilising forces (Figure 4b). Corymbocoumarin however formed stabilizing forces with M^{pro} through carbon hydrogen bond formation with Met165, alkyl hydrophobic interaction with His41, Cys145, Met49, Pro168 and Met165, π-anion interaction with Glu166, π-lone pair interaction with Asn142, π-alkyl interaction with His41 and van der Waals interaction with other residues as shown in Figure 4c. For the above three pyranocoumarins the Δ*G* value from table 1 were ranked with corymbocoumarin (-8.57 kcal/mol) displaying least Δ*G* value, followed by anomalin (-8.18 kcal/mol) and finally seselin with a Δ*G* value of -7.00 kcal/mol. The electrostatic surface potential of the binding site of M^{pro} bound with all the three pyranocoumarins synchronously has been depicted in Figure 5c.

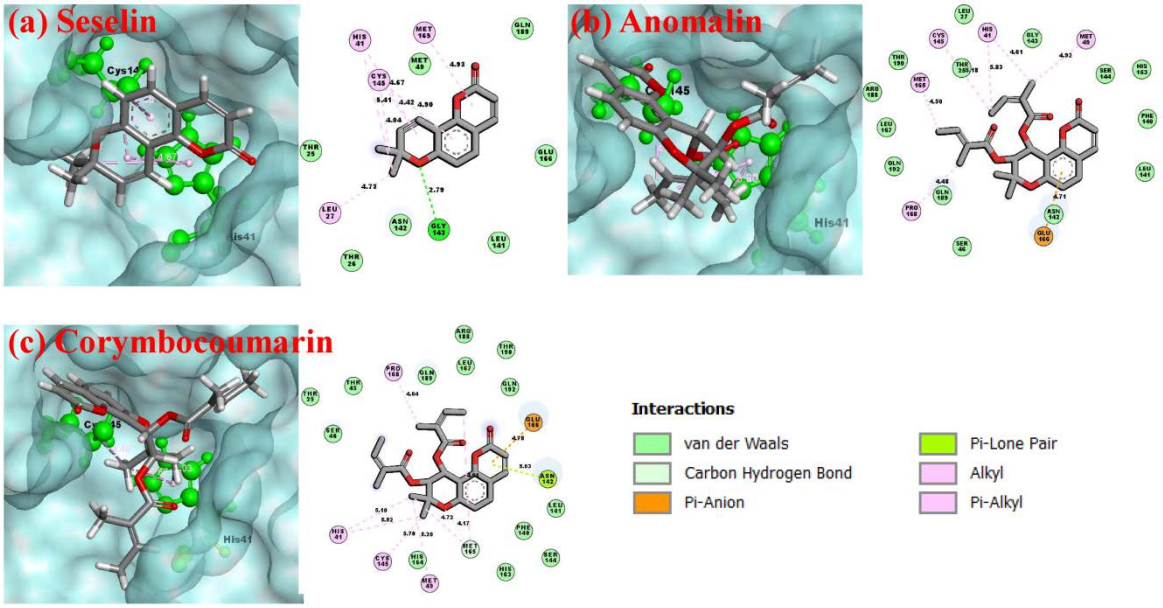

Figure 4.The minimum energy docked poses of the pyranocoumarin derivatives (a) seselin, (b) anomalin and (c) corymbocoumarin with 6Y84 with their corresponding 2-D interaction diagrams.

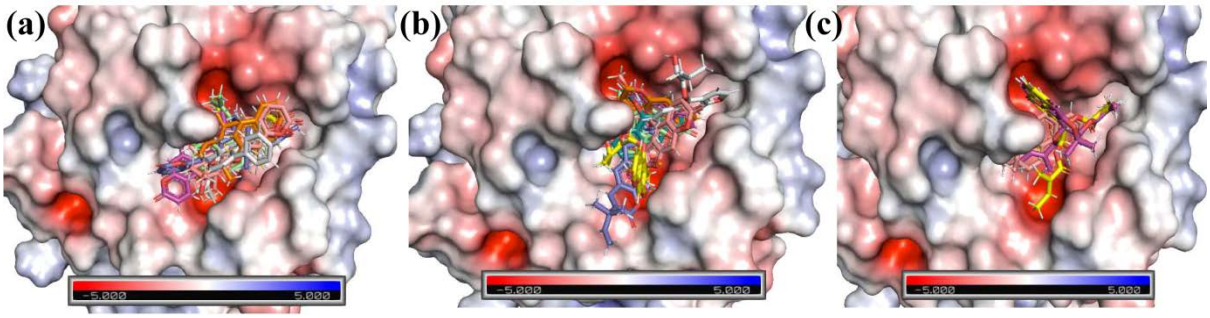

Figure 5. Electrostatic surface representation of the active site of 6Y84 in the presence of (a) simple coumarins, (b) furanocoumarins and (c) pyranocoumarins.

Repurposing or repositioning of many therapeutic drugs is being carried out by many researchers and scientists all over the world as an effective means of treatment against COVID-19. The main protease of SARS-CoV-2, M^{pro}, is a popular target for such studies as inhibition of this enzyme would lead to viral replication coming to a halt. In order to achieve this, blocking the amino acid residues located in the active site of M^{pro} would be required. A recent study on α-ketoamide inhibitors used against SARS-CoV-2 main protease, M^{pro}, revealed that His41, Met49, Gly143, Cys145, His163, His164, Glu166, Pro168, and Gln189

amino acids are the inhibitor binding site residues (Zhang et al., 2020) out of which His41 and Cys145 are known as the catalytic dyad (Jin et al., 2020).

Blind docking studies carried out on three classes of naturally occurring coumarin compounds against the M^{pro} target protein revealed that all the seventeen coumarins which bound to the active site interacted in some manner or another with the above mentioned amino acid residues which suggests that they could impede the proper functioning of the protease. The distance of His41 and Cys145 of each coumarin along with the change in accessible area from the residues located in the active site of M^{pro} has also been represented in Table 2.

Table 2. The distance of the coumarin derivatives from the catalytic site residues His41 and Cys145 along with their ΔASA.

Category	Compounds	Distance (Å)		ΔASA (Å^2)	
		His41	Cys145	His41	Cys145
Simple coumarins	Mesuol	4.84	3.81	21.09	18.61
	Isofraxidin	3.88	3.40	6.90	17.44
	Osthole	4.93	4.84	20.86	21.88
	Methyl galbanate	4.68	4.65	20.64	21.88
	Esculin	2.29	5.61	20.98	21.88
	Kellerin	4.60	4.18	21.09	21.78
Furanocoumarins	Rutamarin	4.60	5.05	21.09	21.88
	Heraclenol	3.49	5.17	21.09	20.69
	Oxypeucedanin	4.92	4.28	21.09	19.60
	Saxalin	5.07	2.44	21.09	21.88
	Pabulenol	2.27	5.74	19.95	19.93
	Pranferol	3.80	3.80	8.72	12.87
	Xanthotoxin	3.01	3.71	20.52	21.88
	Sphondin	2.94	4.38	19.84	21.88
Pyranocoumarins	Seselin	4.67	4.04	20.64	21.88
	Anomalin	3.80	4.22	20.86	21.88
	Corymbocoumarin	4.03	4.40	18.14	20.34

In the structural class of simple coumarins, methylgalbanate was seen to have the lowest energy score, -8.30kcal/mol, compared to the other coumarin compounds, falling within the same class. Under the structural class furanocoumarin, heraclenol had the most negative ΔG

value, -8.20 kcal/mol. This is significant due to the fact that anti-viral properties of herclenol, particularly anti-HIV activity, have been reported in previous studies (Shikishima et al., 2001; Wu et al., 2001). And finally, corymbocoumarin (-8.57 kcal/mol) was ranked with the lowest energy score, among the pyranocoumarin class and also among the other two classes of coumarin compounds. Despite the ΔG values of control drugs such as ritonavir (-9.52 kcal/mol), and lopinavir (-9.00 kcal/mol) when docked with M^{pro} (Das et al., 2020) was more negative than the above mentioned coumarins, however when compared with the Δ*G* of hydroxychloroquine (-7.75 kcal/mol) (Das et al., 2020), a potential drug undergoing assessment for COVID-19 treatment in patients, the coumarin compounds displayed better binding affinity due to their higher negative Δ*G* values. Results from ADME studies (Table S1) also revealed that majority of naturally occurring coumarins, including corymbocoumarin and heraclenol, were highly drug likely due to their non-violation of Lipinski's rule of five as compared to ritonavir (2 violations) and lopinavir (1 violation). Coumarin compounds, due to their natural origin, have many benefits as potential drug candidates due to their low toxicity and least side effects, problems that are faced on administration of most synthetic and semi-synthetic drugs. With this, we can conclude by saying that heraclenol coumarin, in addition to being of natural origin, drug-likely and most importantly, having anti-viral properties, it also displayed a comparable binding energy value with that of methylgalbanate and corymbocoumarin. It could thus be considered a potential SARS-CoV-2 M^{pro} inhibitor but further wet lab studies and investigation needs to be carried out in order to establish it protease inhibiting properties.

4. Conclusion

The rapid spread and transmission of COVID-19 infection across oceans and continents has created a worldwide scare with positive cases and deaths being reported everyday, globally. The lack of effective and fool proof medication as well as broad spectrum inhibitors to control the viral infection through human transmission remains a challenge for researchers

and scientists. At the same time, the development of new anti-viral agents followed by their clinical trials and approval is a time taking process and time is what we do not have. Without a vaccine to prevent COVID-19 infections, the fastest method to treat infected patients has led to repurposing of drugs which are being used for treatments of other existing ailments. As Hippocrates said "Nature itself is the best physician", most drugs being developed today is mainly derived from plant sources. Naturally occurring compounds found in plants are also being screened as an effective treatment against SARS-CoV-2 virus. In this study, naturally occurring coumarin compounds were screened using molecular docking studies against SARS-CoV-2 main protease M^{pro} out of which 17 coumarins could interact with the residues present in the active site of M^{pro}. This interaction could suggest blockage of the active site residues of M^{pro} which are required for proteolytic enzymatic activity to enable viral replication. These potential coumarin protease inhibitors displayed a binding energy score in the range of -6.80 kcal/mol to -8.57 kcal/mol out of which corymbocoumarin (-8.57 kcal/mol), methylgalbanate (8.30 kcal/mol) and hercalenol (8.20 kcal/mol) displayed best negative energy scores from their respective structural classes. The preliminary investigation of these coumarin compounds as potential viral protease inhibitors were carried out using computational methods and further *in vitro* and *in vivo* research work needs to be undertaken to corroborate our findings.

References

Anand, K., Ziebuhr, J., Wadhwani, P., Mesters, J. R., & Hilgenfeld, R. (2003). Coronavirus main proteinase (3CLpro) structure: basis for design of anti-SARS drugs. *Science*, *300*(5626), 1763-1767. https://doi.org/10.1126/science.1085658

BIOVIA., D. (2019). Dassault Systèmes Discovery studio visualizer, 2019 San Diego 2019

Boopathi, S., Poma, A. B., & Kolandaivel, P. (2020). Novel 2019 coronavirus structure, mechanism of action, antiviral drug promises and rule out against its treatment. *Journal of Biomolecular Structure and Dynamics*, 1-10. https://doi.org/10.1080/07391102.2020.1758788

Chan, K. S., Lai, S. T., Chu, C. M., Tsui, E., Tam, C. Y., Wong, M. M., Tse, M. W., Que, T. L., Peiris, J. S., Sung, J., Wong, V. C., & Yuen, K. Y. (2003). Treatment of severe acute respiratory syndrome with lopinavir/ritonavir: a multicentre retrospective matched cohort study. *Hong Kong Med J*, *9*(6), 399-406.

Chu, C. M., Cheng, V. C. C., Hung, I. F. N., Wong, M. M. L., Chan, K. H., Chan, K. S., Kao, R. Y. T., Poon, L. L. M., Wong, C. L. P., Guan, Y., Peiris, J. S. M., Yuen, K. Y., & Group, H. U. S. S. (2004). Role of lopinavir/ritonavir in the treatment of SARS: initial virological and clinical findings. *Thorax*, *59*(3), 252-256. https://doi.org/10.1136/thorax.2003.012658

Cucinotta, D., & Vanelli, M. (2020). WHO Declares COVID-19 a Pandemic. *Acta Biomed*, *91*(1), 157-160. https://doi.org/10.23750/abm.v91i1.9397

Cui, J., Li, F., & Shi, Z. L. (2019). Origin and evolution of pathogenic coronaviruses. *Nat Rev Microbiol*, *17*(3), 181-192. https://doi.org/10.1038/s41579-018-0118-9

Das, S., Sarmah, S., Lyndem, S., & Singha Roy, A. (2020). An investigation into the identification of potential inhibitors of SARS-CoV-2 main protease using molecular docking study. *Journal of Biomolecular Structure and Dynamics*, 1-18. https://doi.org/10.1080/07391102.2020.1763201

Dong, L., Hu, S., & Gao, J. (2020). Discovering drugs to treat coronavirus disease 2019 (COVID-19). *Drug Discov Ther*, *14*(1), 58-60. https://doi.org/10.5582/ddt.2020.01012

Ghannadi, A., Fattahian, K., Shokoohinia, Y., Behbahani, M., & Shahnoush, A. (2014). Anti-Viral Evaluation of Sesquiterpene Coumarins from Ferula assa-foetida against HSV-1. *Iranian journal of pharmaceutical research : IJPR*, *13*(2), 523-530. https://pubmed.ncbi.nlm.nih.gov/25237347

Grosdidier, A., Zoete, V., & Michielin, O. (2011). SwissDock, a protein-small molecule docking web service based on EADock DSS. *Nucleic Acids Res*, *39*(Web Server issue), W270-277. https://doi.org/10.1093/nar/gkr366

Hassan, M. Z., Osman, H., Ali, M. A., & Ahsan, M. J. (2016). Therapeutic potential of coumarins as antiviral agents. *European Journal of Medicinal Chemistry*, *123*, 236-255. https://doi.org/https://doi.org/10.1016/j.ejmech.2016.07.056

Jin, Z., Du, X., Xu, Y., Deng, Y., Liu, M., Zhao, Y., Zhang, B., Li, X., Zhang, L., Peng, C., Duan, Y., Yu, J., Wang, L., Yang, K., Liu, F., Jiang, R., Yang, X., You, T., Liu, X., Yang, X., Bai, F., Liu, H., Liu, X., Guddat, L. W., Xu, W., Xiao, G., Qin, C., Shi, Z., Jiang, H., Rao, Z., & Yang, H. (2020). Structure of Mpro from COVID-19 virus and discovery of its inhibitors. *Nature*. https://doi.org/10.1038/s41586-020-2223-y

Khan, S. A., Zia, K., Ashraf, S., Uddin, R., & Ul-Haq, Z. (2020). Identification of chymotrypsin-like protease inhibitors of SARS-CoV-2 via integrated computational approach. *Journal of Biomolecular Structure and Dynamics*, 1-10. https://doi.org/10.1080/07391102.2020.1751298

Lahlou, M. (2013). The Success of Natural Products in Drug Discovery. *Pharmacology & Pharmacy*, *04*, 17-31. https://doi.org/10.4236/pp.2013.43A003

Li, H., Wang, Y. M., Xu, J. Y., & Cao, B. (2020). [Potential antiviral therapeutics for 2019 Novel Coronavirus]. *Zhonghua Jie He He Hu Xi Za Zhi*, *43*(3), 170-172. https://doi.org/10.3760/cma.j.issn.1001-0939.2020.03.004

Marquez, N., Sancho, R., Bedoya, L. M., Alcami, J., Lopez-Perez, J. L., Feliciano, A. S., Fiebich, B. L., & Munoz, E. (2005). Mesuol, a natural occurring 4-phenylcoumarin, inhibits HIV-1 replication by targeting the NF-kappaB pathway. *Antiviral Res*, *66*(2-3), 137-145. https://doi.org/10.1016/j.antiviral.2005.02.006

Márquez, N., Sancho, R., Bedoya, L. M., Alcamí, J., López-Pérez, J. L., Feliciano, A. S., Fiebich, B. L., & Muñoz, E. (2005). Mesuol, a natural occurring 4-phenylcoumarin, inhibits HIV-1 replication by targeting the NF-κB pathway. *Antiviral Research*, *66*(2), 137-145. https://doi.org/https://doi.org/10.1016/j.antiviral.2005.02.006

Mishra, S., Pandey, A., & Manvati, S. (2020). Coumarin: An emerging antiviral agent. *Heliyon*, *6*(1), e03217-e03217. https://doi.org/10.1016/j.heliyon.2020.e03217

Morse, J. S., Lalonde, T., Xu, S., & Liu, W. R. (2020). Learning from the Past: Possible Urgent Prevention and Treatment Options for Severe Acute Respiratory Infections Caused by 2019-nCoV. *21*(5), 730-738. https://doi.org/10.1002/cbic.202000047

Muralidharan, N., Sakthivel, R., Velmurugan, D., & Gromiha, M. M. (2020). Computational studies of drug repurposing and synergism of lopinavir, oseltamivir and ritonavir binding with SARS-CoV-2 protease against COVID-19. *Journal of Biomolecular Structure and Dynamics*, 1-6. https://doi.org/10.1080/07391102.2020.1752802

Owen, C. D., Lukacik, P., Strain-Damerell, C.M., Douangamath, A., Powell, A.J., Fearon, D., Brandao-Neto, J., Crawshaw, A.D., Aragao, D., Williams, M., Flaig, R., Hall, D., McAauley, K., Stuart, D.I., von Delft, F., Walsh, M.A. (2020). COVID-19 main protease with unliganded

active site (2019-nCoV, coronavirus disease 2019, SARS-CoV-2). *RCSB Protein Data Bank ID 6Y84 2020*, 3–7. https://doi.org/10.2210/pdb6Y84.

Pettersen, E. F., Goddard, T. D., Huang, C. C., Couch, G. S., Greenblatt, D. M., Meng, E. C., & Ferrin, T. E. (2004). UCSF Chimera--a visualization system for exploratory research and analysis. *J Comput Chem*, *25*(13), 1605-1612. https://doi.org/10.1002/jcc.20084

Schrodinger, L. (2017). The PyMOL Molecular Graphics System, Version 2.0 2017.

Shikishima, Y., Takaishi, Y., Honda, G., Ito, M., Takfda, Y., Kodzhimatov, O. K., Ashurmetov, O., & Lee, K. H. (2001). Chemical constituents of Prangos tschiniganica; structure elucidation and absolute configuration of coumarin and furanocoumarin derivatives with anti-HIV activity. *Chem Pharm Bull (Tokyo)*, *49*(7), 877-880. https://doi.org/10.1248/cpb.49.877

Wang, C., Horby, P. W., Hayden, F. G., & Gao, G. F. (2020). A novel coronavirus outbreak of global health concern. *Lancet*, *395*(10223), 470-473. https://doi.org/10.1016/s0140-6736(20)30185-9

Wang H, L. X., Yao H, Feng J, Liu R. (2009). Research progress on application of coumarin and its derivatives. *Chemical Industry Times*, *23*(8), 40-43.

Wu, T. S., Tsang, Z. J., Wu, P. L., Lin, F. W., Li, C. Y., Teng, C. M., & Lee, K. H. (2001). New constituents and antiplatelet aggregation and anti-HIV principles of Artemisia capillaris. *Bioorg Med Chem*, *9*(1), 77-83. https://doi.org/10.1016/s0968-0896(00)00225-x

Wu Y-S, L. W.-H., T.-A.Hsu J, Hsieh H-P. (2006). Antiviral Drug Discovery Against SARS-CoV. *Curr Med Chem 13*, 2003–2020. https://doi.org/doi.org/10.2174/092986706777584988.

Xu, B., Wang, L., Gonzalez-Molleda, L., Wang, Y., Xu, J., & Yuan, Y. (2014). Antiviral activity of (+)-rutamarin against Kaposi's sarcoma-associated herpesvirus by inhibition of the catalytic activity of human topoisomerase II. *Antimicrob Agents Chemother*, *58*(1), 563-573. https://doi.org/10.1128/aac.01259-13

Zhang, L., Lin, D., Sun, X., Curth, U., Drosten, C., Sauerhering, L., Becker, S., Rox, K., & Hilgenfeld, R. (2020). Crystal structure of SARS-CoV-2 main protease provides a basis for design of improved α-ketoamide inhibitors. *368*(6489), 409-412. https://doi.org/10.1126/science.abb3405 %J Science

Zhou, P., Takaishi, Y., Duan, H., Chen, B., Honda, G., Itoh, M., Takeda, Y., Kodzhimatov, O. K., & Lee, K.-H. (2000). Coumarins and bicoumarin from Ferula sumbul: anti-HIV activity and inhibition of cytokine release. *Phytochemistry*, *53*(6), 689-697. https://doi.org/https://doi.org/10.1016/S0031-9422(99)00554-3

In silico screening of naturally occurring coumarin derivatives for the inhibition of the main protease of SARS-CoV-2

Sona Lyndem[$], Sharat Sarmah[$], Sourav Das and Atanu Singha Roy*

Department of Chemistry, National Institute of Technology Meghalaya, Shillong 793003, India

[$] Equal contribution

Running head title: Coumarins as potential inhibitors of SARS-CoV-2

***Corresponding Author:** Atanu Singha Roy

Tel.: +91 364−2501294

Fax: +91 364−2501113

Email: singharoyatanu@gmail.com; asroy86@nitm.ac.in

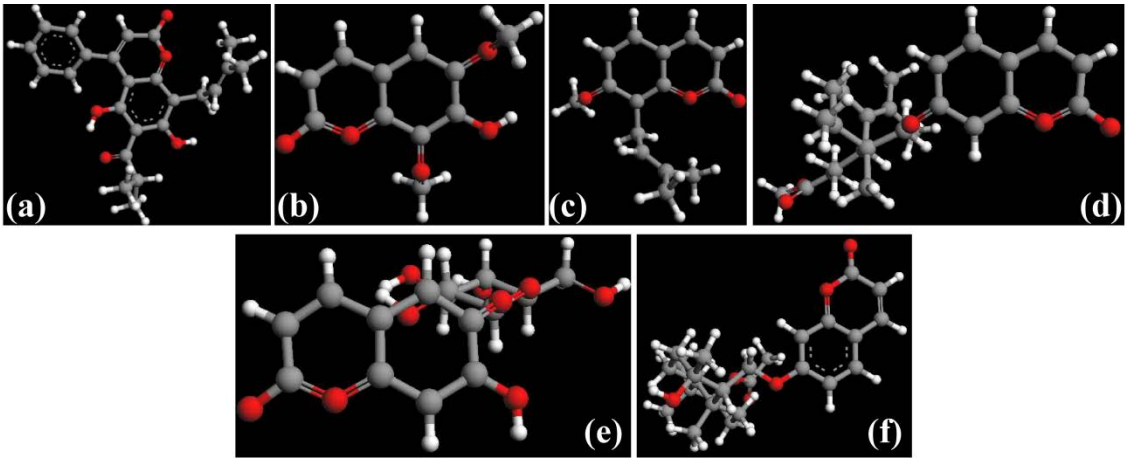

Figure S1. The optimized structure of simple coumarin derivatives (a) mesuol, (b) isofraxidin, (c) osthole, (d) methylgalbanate, (e) esculin and (f) kellerin obtained from ArgusLab using PM3 method.

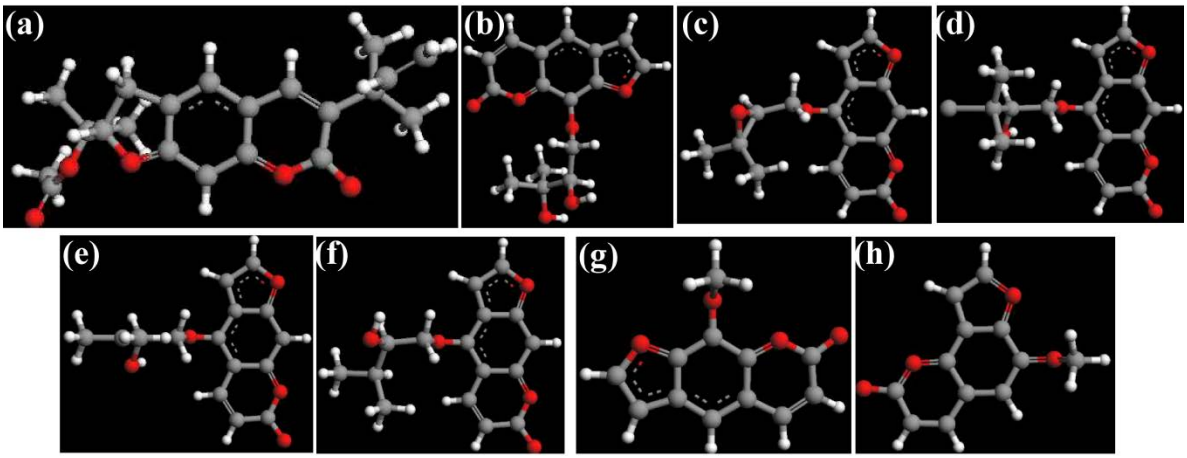

Figure S2. The optimized structure of furanocoumarin derivatives (a) rutamarin, (b) heraclenol, (c) oxypeucedanin, (d) saxalin, (e) pabulenol, (f) pranferol,(g) xanthotoxin and (h) sphondin obtained from ArgusLab using PM3 method

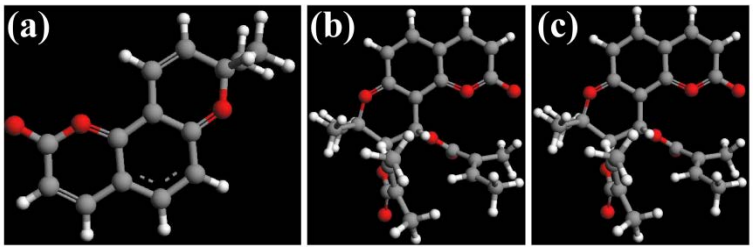

Figure S3. The optimized structure of pyranocoumarin derivatives (a) seselin, (b) anomalin and (c) corymbocoumarin obtained from ArgusLab using PM3 method.

Table S1. The chemical structures, natural sources and physicochemical properties of the coumarin derivatives.

Sl. No	Compound	Sources	Molecular Structure	Lipinski's Rule of Five	
				Properties	**Value**
1	Mesuol	*Marila pluricostata* (Marquez et al., 2005)	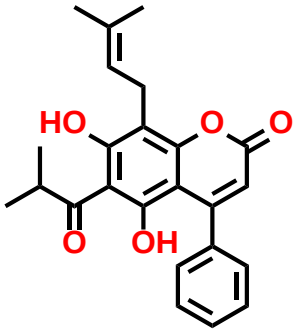	Molecular weight (<500Da)	392.44
				LogP (<5)	5.22
				H-Bond donor (<5)	2
				H-Bond acceptor (<10)	5
				Violations	1
2	Isofraxidin	*Eleutherococcus senticosus,* (Majnooni MB, 2020) *Artemisia abrotanum L* (Cubukcu et al., 1990)	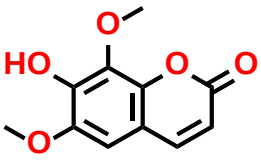	Molecular weight (<500Da)	222.19
				LogP (<5)	1.52
				H-Bond donor (<5)	1
				H-Bond acceptor (<10)	5
				Violations	Nil
3	Osthole	*Cnidium monnieri,* (Zhang et al., 2015)	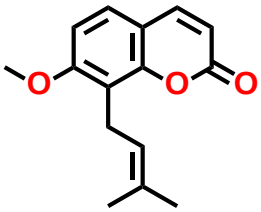	Molecular weight (<500Da)	244.29
				LogP (<5)	3.31
				H-Bond donor (<5)	0
				H-Bond acceptor (<10)	3
				Violations	Nil
4	Methyl galbanate	*Ferula szowitsiana* (Kohno et al., 2011)	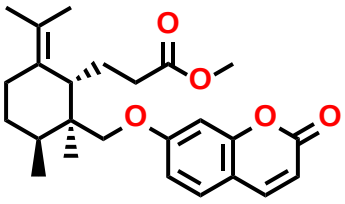	Molecular weight (<500Da)	412.52
				LogP (<5)	5.51
				H-Bond donor (<5)	0
				H-Bond acceptor (<10)	5
				Violations	1
5	Esculin	*Lactuca virosa, Ocimum basilicum* (Maria João Matos, 2015)	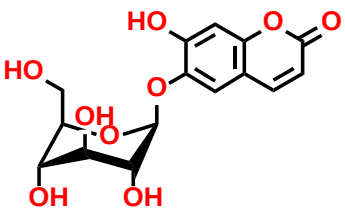	Molecular weight (<500Da)	340.28
				LogP (<5)	-1.32
				H-Bond donor (<5)	5
				H-Bond acceptor (<10)	9
				Violations	Nil

6	Kellerin	*Ferula asafoetida* (Ghannadi et al., 2014)	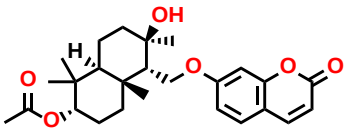	Molecular weight (<500Da)	442.54
				LogP (<5)	4.71
				H-Bond donor (<5)	1
				H-Bond acceptor (<10)	6
				Violations	Nil
7	Rutamarin	*Rutagraveolens* (Xu et al., 2014)	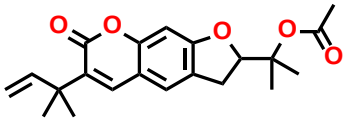	Molecular weight (<500Da)	356.41
				LogP (<5)	3.90
				H-Bond donor (<5)	0
				H-Bond acceptor (<10)	5
				Violations	Nil
8	Heraclenol	*Ferula sumbul (Zhou et al., 2000), Oppopanax chironium* (Appendino et al., 2004)	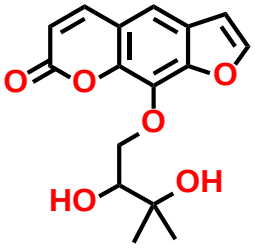	Molecular weight (<500Da)	304.29
				LogP (<5)	2.05
				H-Bond donor (<5)	2
				H-Bond acceptor (<10)	6
				Violations	Nil
9	Oxypeucedanin	*Ferula sumbul (Zhou et al., 2000), Angelica archangelica* (Newall, 1996)	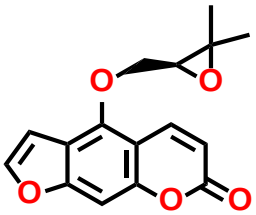	Molecular weight (<500Da)	286.28
				LogP (<5)	3.10
				H-Bond donor (<5)	0
				H-Bond acceptor (<10)	5
				Violations	Nil
10	Saxalin	*Prangos tschimganica* (Shikishima et al., 2001)	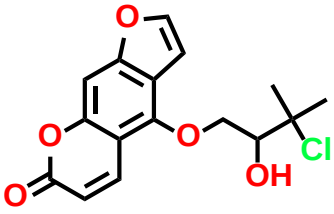	Molecular weight (<500Da)	322.74
				LogP (<5)	3.30
				H-Bond donor (<5)	1
				H-Bond acceptor (<10)	5
				Violations	Nil
11	Pabulenol	*Prangos tschimganica* (Shikishima et al., 2001)	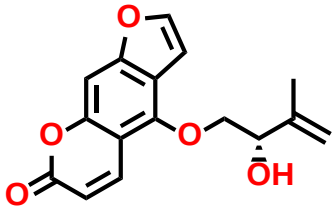	Molecular weight (<500Da)	286.28
				LogP (<5)	2.86
				H-Bond donor (<5)	1
				H-Bond acceptor (<10)	5
				Violations	Nil

12	Pranferol	*Ferula sumbul* (Zhou et al., 2000)	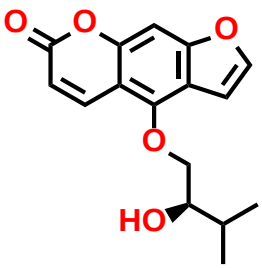	Molecular weight (<500Da)	288.30
				LogP (<5)	2.71
				H-Bond donor (<5)	1
				H-Bond acceptor (<10)	5
				Violations	Nil
13	Xanthotoxin	*Ferula sumbul (Zhou et al., 2000), Angelica archangelica* (Newall, 1996)	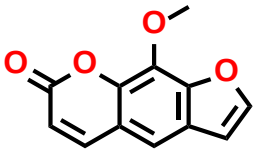	Molecular weight (<500Da)	216.19
				LogP (<5)	2.55
				H-Bond donor (<5)	0
				H-Bond acceptor (<10)	4
				Violations	Nil
14	Sphondin	*Heracleum laciniatum* (Yang et al., 2002)	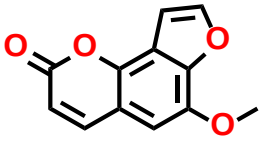	Molecular weight (<500Da)	216.19
				LogP (<5)	2.55
				H-Bond donor (<5)	0
				H-Bond acceptor (<10)	4
				Violations	Nil
15	Seselin	*Apiumgraveolens (Newall, 1996), Foeniculum vulgare* (M. Khan, 2014)	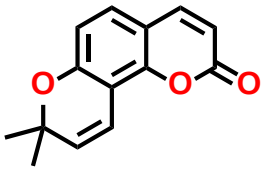	Molecular weight (<500Da)	228.24
				LogP (<5)	2.87
				H-Bond donor (<5)	0
				H-Bond acceptor (<10)	3
				Violations	Nil
16	Anomalin	*Saposhnikovia divaricate* (S. Khan et al., 2011)	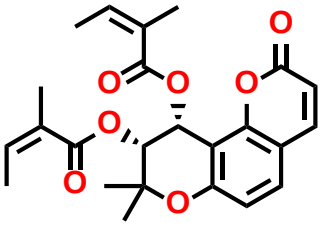	Molecular weight (<500Da)	274.23
				LogP (<5)	2.08
				H-Bond donor (<5)	4
				H-Bond acceptor (<10)	6
				Violations	Nil
17	Corymbocoumarin	*Seseli gummniferum* (Chun et al., 2016)	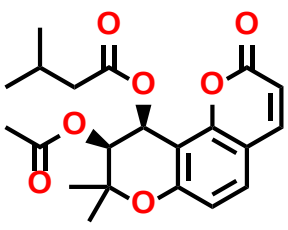	Molecular weight (<500Da)	388.41
				LogP (<5)	3.20
				H-Bond donor (<5)	0
				H-Bond acceptor (<10)	7
				Violations	Nil

References

Appendino, G., Bianchi, F., Bader, A., Campagnuolo, C., Fattorusso, E., Taglialatela-Scafati, O., Blanco-Molina, M., Macho, A., Fiebich, B. L., Bremner, P., Heinrich, M., Ballero, M., & Munoz, E. (2004). Coumarins from Opopanax chironium. New dihydrofuranocoumarins and differential induction of apoptosis by imperatorin and heraclenin. *J Nat Prod*, *67*(4), 532-536. https://doi.org/10.1021/np0340652

Chun, J., Tosun, A., & Kim, Y. S. (2016). Anti-inflammatory effect of corymbocoumarin from Seseli gummiferum subsp. corymbosum through suppression of NF-kappaB signaling pathway and induction of HO-1 expression in LPS-stimulated RAW 264.7 cells. *Int Immunopharmacol*, *31*, 207-215. https://doi.org/10.1016/j.intimp.2015.12.029

Cubukcu, B., Bray, D. H., Warhurst, D. C., Mericli, A. H., Ozhatay, N., & Sariyar, G. (1990). In vitro antimalarial activity of crude extracts and compounds from Artemisia abrotanum L. *4*(5), 203-204. https://doi.org/10.1002/ptr.2650040510

Ghannadi, A., Fattahian, K., Shokoohinia, Y., Behbahani, M., & Shahnoush, A. (2014). Anti-Viral Evaluation of Sesquiterpene Coumarins from Ferula assa-foetida against HSV-1. *Iranian journal of pharmaceutical research : IJPR*, *13*(2), 523-530. https://pubmed.ncbi.nlm.nih.gov/25237347

Khan, M. (2014). Foeniculum vulgare Mill. A Medicinal Herb. *Medicinal Plant Research*, *4*. https://doi.org/10.5376/mpr.2014.04.0006

Khan, S., Shin, E. M., Choi, R. J., Jung, Y. H., Kim, J., Tosun, A., & Kim, Y. S. (2011). Suppression of LPS-induced inflammatory and NF-kappaB responses by anomalin in RAW 264.7 macrophages. *J Cell Biochem*, *112*(8), 2179-2188. https://doi.org/10.1002/jcb.23137

Kohno, S., Murata, T., Sugiura, A., Ito, C., Iranshahi, M., Hikita, K., & Kaneda, N. (2011). Methyl galbanate, a novel inhibitor of nitric oxide production in mouse macrophage RAW264.7 cells. *Journal of Natural Medicines*, *65*(2), 353-359. https://doi.org/10.1007/s11418-010-0505-7

Majnooni MB, F. S., Shokoohinia Y, Mojarrab M, Kazemi-Afrakoti S, Farzaei MH. (2020). Isofraxidin: Synthesis, Biosynthesis, Isolation, Pharmacokinetic and Pharmacological Properties. *Molecules*, *25*(9), 2040. https://doi.org/doi.org/10.3390/molecules25092040

Maria João Matos, L. S., Eugenio Uriarte, Orlando A. Abreu, Enrique Molina and Estela Guardado Yordi. (2015). *Coumarins — An Important Class of Phytochemicals* (A. V. R. a. L. G. Rao, Ed.). https://doi.org/DOI: 10.5772/59982

Marquez, N., Sancho, R., Bedoya, L. M., Alcami, J., Lopez-Perez, J. L., Feliciano, A. S., Fiebich, B. L., & Munoz, E. (2005). Mesuol, a natural occurring 4-phenylcoumarin, inhibits HIV-1 replication by targeting the NF-kappaB pathway. *Antiviral Res*, *66*(2-3), 137-145. https://doi.org/10.1016/j.antiviral.2005.02.006

Newall, C. A. (1996). Herbal medicines : a guide for health-care professionals. In L. A. Anderson & J. D. Phillipson (Eds.). Pharmaceutical Press.

Shikishima, Y., Takaishi, Y., Honda, G., Ito, M., Takfda, Y., Kodzhimatov, O. K., Ashurmetov, O., & Lee, K. H. (2001). Chemical constituents of Prangos tschiniganica; structure elucidation and absolute configuration of coumarin and furanocoumarin derivatives with anti-HIV activity. *Chem Pharm Bull (Tokyo)*, *49*(7), 877-880. https://doi.org/10.1248/cpb.49.877

Xu, B., Wang, L., Gonzalez-Molleda, L., Wang, Y., Xu, J., & Yuan, Y. (2014). Antiviral activity of (+)-rutamarin against Kaposi's sarcoma-associated herpesvirus by inhibition of the catalytic activity of human topoisomerase II. *Antimicrob Agents Chemother*, *58*(1), 563-573. https://doi.org/10.1128/aac.01259-13

Yang, L. L., Liang, Y. C., Chang, C. W., Lee, W. S., Kuo, C. T., Wang, C. C., Lee, H. M., & Lin, C. H. (2002). Effects of sphondin, isolated from Heracleum laciniatum, on IL-1beta-induced cyclooxygenase-2 expression in human pulmonary epithelial cells. *Life Sci*, *72*(2), 199-213. https://doi.org/10.1016/s0024-3205(02)02173-2

Zhang, Z.-R., Leung, W. N., Cheung, H. Y., & Chan, C. W. (2015). Osthole: A Review on Its Bioactivities, Pharmacological Properties, and Potential as Alternative Medicine. *Evidence-based complementary and alternative medicine : eCAM*, *2015*, 919616-919616. https://doi.org/10.1155/2015/919616

Zhou, P., Takaishi, Y., Duan, H., Chen, B., Honda, G., Itoh, M., Takeda, Y., Kodzhimatov, O. K., & Lee, K.-H. (2000). Coumarins and bicoumarin from Ferula sumbul: anti-HIV activity and inhibition of cytokine release. *Phytochemistry*, *53*(6), 689-697. https://doi.org/https://doi.org/10.1016/S0031-9422(99)00554-3